Title
Electronic structure of correlated electron materials from photoemission in high-quality single crystals

Authors
Arko, AJ
Joyce, JJ
Moore, DP
et al.

Publication Date
2001-06-01

DOI
10.1016/s0368-2048(01)00256-0

ELSEVIER

JOURNAL OF ELECTRON SPECTROSCOPY and Related Phenomena

Journal of Electron Spectroscopy and Related Phenomena 117–118 (2001) 323–345

www.elsevier.nl/locate/elspec

Electronic structure of correlated electron materials from photoemission in high-quality single crystals

A.J. Arko[a,*], J.J. Joyce[a], D.P. Moore[a], J.L. Sarrao[a], L. Morales[a], T. Durakiewicz[a], Z. Fisk[a], D.D. Koelling[b], C.G. Olson[c]

[a] *MST-10 Group, Los Alamos National Laboratory, Mail Stop K764, Los Alamos, NM 87545, USA*
[b] *Argonne National Laboratory, Argonne, IL 60439, USA*
[c] *Iowa State University, Ames, IA, USA*

Received 18 August 2000; accepted 4 December 2000

Abstract

Much of our understanding of heavy fermion systems over the past two decades has been based on the single impurity model and its approximate solutions. We show with numerous examples of photoelectron spectra, especially with $YbInCu_4$, that this model is not applicable to stoichiometric heavy fermion compounds. There is overwhelming evidence that the correct description of heavy fermions must include very narrow, hybridized bands which exist already at temperatures far above the thermodynamically determined Kondo temperature, and that these bands are relatively temperature independent. Some form of the periodic Anderson model (PAM) is needed, one which results in very narrow renormalized LDA bands. We compare our data to one form of the PAM.

Keywords: Heavy fermion systems; Photoelectron spectra; Periodic Anderson model; Single impurity model

1. Introduction

Since their discovery in the mid-seventies [1,2], the unusual properties of heavy fermions have sparked an avalanche of research over the last two decades. The reader is referred to numerous review articles [3–9]. The term heavy fermion refers to materials (primarily compounds with elements having an unfilled 4f or 5f shell) whose electronic properties suggest that the conduction electrons have a very heavy effective mass. deHaas–van Alphen measurements have confirmed the existence of heavy masses [10–12]. It is also well established that indeed it is the f-electrons that are responsible for the unusual properties [4].

Magnetic susceptibility (χ) measurements of heavy fermion compounds generally yield a Curie–Weiss behavior at high temperatures consistent with a well-developed moment (see, for example, Ref. [8]). Indeed, the f-electrons appear to behave as non-interacting single impurities at elevated temperature, a fact that has promoted an almost religious belief in the so-called single impurity model, or SIM [13]. Below some characteristic temperature, usually referred to as the Kondo temperature or T_K, the susceptibility levels off or even decreases. This is interpreted as a compensation of the magnetic moment by the ligand conduction electrons that are

*Corresponding author. Tel.: +1-505-665-7652; fax: +1-505-665-0758.
E-mail address: arko@lanl.gov (A.J. Arko).

0368-2048/01/$ – see front matter
PII: S0368-2048(01)00256-0

believed to align anti-parallel to the f-electrons to form a singlet state (see, e.g. Ref. [4]). Within the SIM, the slight hybridization with these ligand electrons pulls some f-DOS to the Fermi energy, E_F, and results in a sharp itinerant resonant state called the Kondo resonance, or KR. At still lower temperatures, a dramatic drop in the electrical resistivity, ρ, is interpreted [3] as due to the formation of a coherent periodic lattice of the KR, called the Kondo lattice, where a heavy crystalline mass develops. The concept of a Kondo or Anderson lattice appears to date back to Lawrence et al. [14], but the reader is referred also to an excellent review of theoretical approaches by Lee et al. [13].

There is, however, another school of thought that claims that the f-electrons form well-defined Bloch states and very narrow bands at all temperatures [15–17]. Conventional band theory (i.e. the local density approximation, or LDA), however, is unable to explain the high-temperature properties as well as the very heavy mass. Renormalized band theory may yet prove useful. However, the success of the SIM in explaining macroscopic bulk phenomena suggests a correctness, at least at some level even if it is only self-consistent. It is our contention that the resolution of the problem will lie in the combining of some form of the periodic Anderson model (PAM) with LDA.

By far and away the most comprehensive and widely accepted model of heavy fermion electronic structure is the Gunnarsson and Schonhammer approximate solution of SIM [18,19], together with the non-crossing approximation, or NCA [20–22]. Several other treatments are also available, but a universal behavior for the f-electron DOS that comes out of all these approximate solutions is the prediction of scaling of its properties with T_K.

While heavy fermion behavior is found in Ce, Yb, U, and other transuranic compounds, NCA is strictly applicable only to Ce (one electron) and Yb (one hole) compounds. PAM in its present form [23,24] is even more restrictive, being applicable only to the one f-electron case, but this is primarily a consequence of complexity rather than a fundamental difficulty. Indeed, it is generally accepted that NCA fails for open f-shells containing more than one f-electron (e.g. uranium). This situation seems highly undesirable and artificial. It is counter-intuitive to accept the notion that entirely similar heavy fermion behavior in different materials requires different models. Towards this end, the PAM offers the possibility of extension to more than one f-electron, while NCA is already accepted as failing for the case of uranium.

Photoelectron spectroscopy (PES) and the even more detailed angle resolved PES or ARPES, constitute the most direct measurement of the electronic structure of a material. Indeed, PES measurements on heavy fermions have been abundant (see Refs. [9,25], and references therein) owing to the very specific predictions of the GS and NCA regarding the width, position, spectral weight, and temperature dependence of the f-electron DOS. Much of the early PES work was performed on poly-crystalline samples, scraped in situ to expose a clean surface. Often, good agreement with the GS approximation was reported [9,25–43]. But while early PES measurements suffered from poor sample quality and sometimes poor resolution, today's equipment and high quality crystals are more than adequate to test NCA. The bulk of the single crystal work was performed by our own Los Alamos group [24,44–48].

In order to test the applicability of NCA to heavy fermions it is important to note that NCA predicts complete particle-hole symmetry such that PES spectrum for occupied states in Ce (one electron) should bear a resemblance to the spectrum of empty states in Yb (one hole) and vice versa. This latter prediction is crucial since, unlike in Ce where the KR is predicted to peak at $k_B T_K$ above E_F in the empty states, in Yb it is predicted to peak at $k_B T_K$ below E_F and is thus fully occupied. The full power and high resolution of PES (vs. BIS) can now be utilized at high intensity synchrotron beamlines, at photon energies which maximize 4f PES cross sections [49]. Thus one may relatively easily measure the 4f temperature dependence, making Yb compounds the materials of choice for testing the SIM via PES. Indeed, for this test, $YbInCu_4$ is unique, owing to its isostructural phase transition at $T_V = 40$ K whereby T_K changes from 400 K below T_V to 30 K above T_V.

In spite of the appeal of Yb compounds, most previous investigations have concentrated on Ce heavy fermion compounds (Refs. [25–43] are representative) in which a measurement of the tempera-

ture dependence is complicated by the sampling of the presumably intense KR above E_F as the Fermi function broadens with temperature [44]. Additionally any satellite or surface features are degenerate with bulk features. For these reasons one generally finds that, in order to test the SIM, only parameter manipulation within NCA is performed [25–43] until the parametrized Ce compound PES spectrum bears a resemblance to the measured spectrum. Although Yb heavy fermion compounds are the obvious choice for an accurate study of NCA applicability, investigations of Yb compounds are strangely sparse or are flawed by use of sintered or poly-crystalline specimens. Occasionally single crystal samples are utilized but the surfaces are nonetheless prepared by scraping. Measurement of cleaved single crystal surfaces of Yb compounds has been primarily utilized by the Los Alamos group [24,44–48].

In this manuscript, then, we primarily report PES measurements on stoichiometric single crystal compounds, and point out the serious disagreements with GS and NCA. In many materials band formation far above T_K is evident thus pointing to the need for periodic models such as PAM. This is especially true in uranium compounds where p–f or d–f hybridized bands are unmistakable.

2. Experimental

Most of the measurements were performed at the Synchrotron Radiation Center of the University of Wisconsin. The latest data (3-dimensional plots of uranium compounds and $YbInCu_4$) were collected using the two dimensional capability of the Scienta analyzer and the PGM beamline. At 60 eV photon energy the instrument resolution was better than 25 meV. The earlier data was obtained using an HA50 VSW analyzer with typically 75 meV resolution. In all cases the background chamber pressure was in the 10^{-11} Torr range. Single crystal samples were cleaved in situ at typically 20 K and measured at 20 K (unless otherwise indicated).

In presenting the spectra, for purposes of brevity, we often refer to the near-E_F feature as either the $4f_{5/2}$ peak in Ce or the $4f_{7/2}$ peak in Yb compounds, rather than the Kondo resonance, or KR. The spin–orbit split sideband is referred to as the $4f_{7/2}$ peak in Ce and as the $4f_{5/2}$ peak in Yb. If we indeed have hybridized band formation, as we hope to show, we realize that such a separation is not strictly correct.

3. Single crystal vs. poly-crystal PES

As stated above, much of the early PES work on heavy fermions was performed on scraped poly-crystalline samples. Agreement with GS and NCA was generally reported [25–43]. With the advent of single crystals, however, this agreement dissipated. It was found that poly-crystals, particularly those scraped to produce a clean surface, yielded a very weak intensity at E_F relative to single crystals. This occurs both in Yb and Ce heavy fermions. In Fig. 1, a comparison is made [24] between single- and poly-crystalline $YbCu_2Si_2$, both specimens cleaved (not scraped) in situ at 20 K, and measured at 20 K ($T_K \sim 35$ K). The spectra have been normalized so

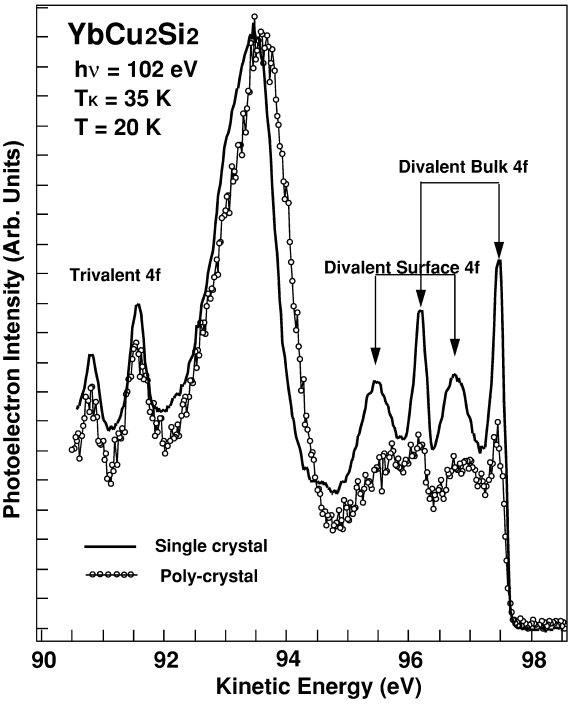

Fig. 1. Comparison of PES spectra for single crystal and poly crystal $YbCu_2Si_2$. While the trivalent 4f features and the Cu3d peak are normalized well to each other, the divalent features suffer a dramatic loss of intensity when long range order is missing.

that the trivalent portion of the spectrum in the −5 to −12 eV range (presumed to be entirely due to the bulk) has equal intensities in both curves when measured peak to valley. While the Cu3d features at −4 eV below E_F normalize in this way to equal intensity in both materials (the slight shifts are due to angle resolved effects), the bulk divalent portion of the Yb-4f spectrum within 2 eV of the Fermi energy is dramatically reduced in the poly-crystalline sample. The exact nature of this phenomenon is not fully understood, but it surely resides in the requirement for long range order near the surface to obtain the full intensity of the near-E_F features. An isolated impurity would not suffer from lack of long range order. This would already seem to point toward a narrow band-like nature of these features, and the need for a periodic model such as PAM to model them.

Scraping of surfaces, whether single crystals or poly crystals, has also been shown to have a deleterious effect on the bulk divalent intensity. An experiment by the Los Alamos group on polycrystalline $YbAgCu_4$ yielded the result [24] that the scraping of the surface completely eliminated the bulk and surface $4f_{5/2}$ peaks. While this might be interpreted as indicating the existence of a subsurface layer, it is also fully consistent with the notion of loss of long range order and hence coherence of narrow bands. The notion of a subsurface, however, has been negated repeatedly by Joyce et al. [46] who studied a number of Yb compounds at XPS energies where the escape depth of photoelectrons is much longer. This subject will be dealt with in greater detail below in connection with $YbInCu_4$.

4. Lack of scaling with T_K in Ce compounds

Perhaps the single most important prediction of the GS and NCA is that of scaling of the various spectral properties with T_K, the universal parameter. In particular, the spectral weight, position, and width of the $4f_{5/2}$ state in Ce are predicted to scale with T_K. While early PES results were generally reported to be in exact agreement with GS and NCA for several materials, this all changed with single crystals.

Arko et al. [24] pointed out that by using high quality single crystals one obtains an amazing similarity in Ce heavy fermion spectra, regardless of T_K. This can be seen in Fig. 2 (taken from Ref. [24]) where spectra for seven Ce heavy fermions (including two directions for $CeBe_{13}$) are plotted. One observes the interesting effect that spectral differences with momentum within the same crystal ($CeBe_{13}$) are in fact larger than differences between materials whose T_K values differ by as much as two orders of magnitude. All the spectra in Fig. 2 were taken at a photon energy of 120 eV which roughly corresponds to the 4d absorption edge and thus resonantly enhances the 4f emission. The energy

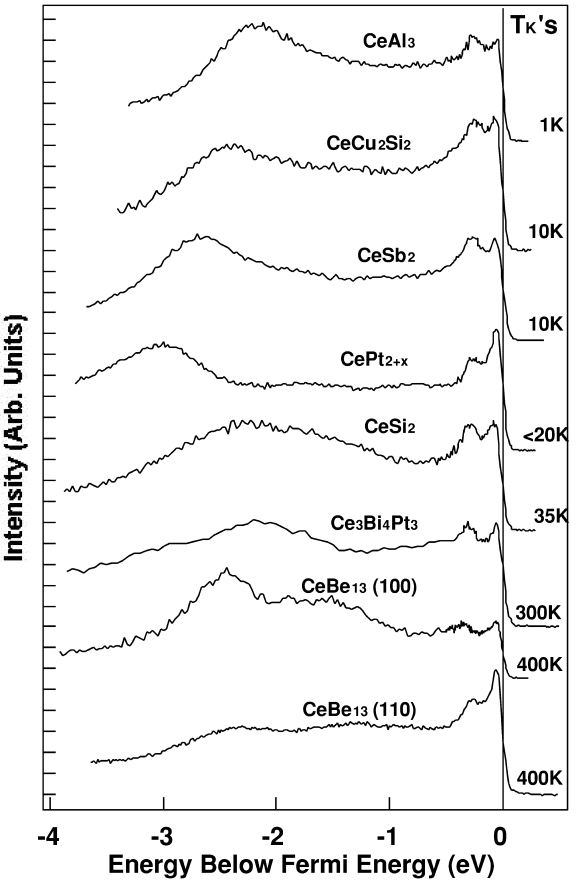

Fig. 2. PES spectra for a number of Ce heavy fermions with T_Ks varying by two orders of magnitude, taken at $h\nu = 120$ eV and 20 K to test for the scaling with T_K. The near-E_F features show a greater difference between two directions within the same crystal ($CeBe_{13}$) than between two materials whose T_Ks differ by a factor of 400 K.

resolution in each case is about 90 meV. All spectra represent raw data except in the case of $CeCu_2Si_2$ where the spectrum at anti-resonance ($h\nu = 112$ eV) has been subtracted from the resonance spectrum in order to eliminate the very strong Cu3d emission. In Fig. 2 one should further note that $CeAl_3$ and $CeSi_2$ are cleaved poly-crystals, with single crystals not available. Further, it should be pointed out that in some materials (e.g. $CeIn_3$, or $CeRh_2Si_2$, recently measured by the Los Alamos group but not published) no 4f-weight is found at the Fermi energy despite a $T_K > 10$ K. This adds further confusion to the scaling law since a relatively large $4f_{5/2}$ spectral intensity exists [24] in $CeAl_2$, previously considered as the quintessential trivalent Ce compound [9]. We have the situation that a smaller T_K yields a larger $4f_{5/2}$ peak.

The point to remember from Fig. 2 is that the spectral weights of the $4f_{5/2}$ features do not monotonically increase with T_K so that one is forced to the conclusion that there is no apparent scaling of the $4f_{5/2}$ spectral weights with T_K. This lack of scaling cannot be accounted for by inclusion of f^2 intensity (i.e. doubly occupied f-state) originating from finite Coulomb correlation (U_{ff}) effects, since the f^2 DOS, if present, is broad and featureless and hence cannot change the relative amplitudes of the occupied states. Nor can one resort to a lowering of the $4f_{5/2}$ degeneracy to $N_f = 2$ (from 6) by the introduction of two additional crystal field (CF) levels, since, as previously shown by Joyce and Arko [50], even in the presence of these CF states the GS and NCA models still predict a scaling of the $4f_{5/2}$ spectral weight with T_K (As an aside we would point out that CF states have never been observed in PES despite more than adequate resolution and low temperatures). The scaling problems, particularly the lack of $4f_{5/2}$ intensity in some compounds with a relatively high T_K, may be rooted in more fundamental photoemission selection rules. Investigations are currently underway to resolve this issue. In any case, however, they point to a fundamental flaw in the SIM.

5. Fermi statistics and phonon broadening

Temperature dependence of the KR spectral weight ranks as the second most important prediction of NCA. Indeed, to paraphrase [39], a failure to find the scaling and the temperature dependence should be sufficient to abandon the SIM. In single crystal PES for all correlated electron systems, any temperature dependence is completely accounted for by the conventional effects of Fermi function truncation (i.e. Fermi statistics) and phonon broadening, without any need for NCA effects [46]. That this broadening is present (to the tune of about 100 meV at 300 K in nearly all systems) will become clear in the discussion of $YbInCu_4$, below. Here we first show that Ce compounds can likewise be explained in this way.

In Fig. 3 the spectra at resonance for $CeBe_{13}$ are shown with 90 meV resolution at 20 and 300 K (from Ref. [44]). In this figure the 20 K spectrum is first fitted with a symmetric Lorentzian centered at -20 meV for the $4f_{5/2}$ state and a Gaussian peak at -280 meV to simulate the $4f_{7/2}$ feature. This assumes that

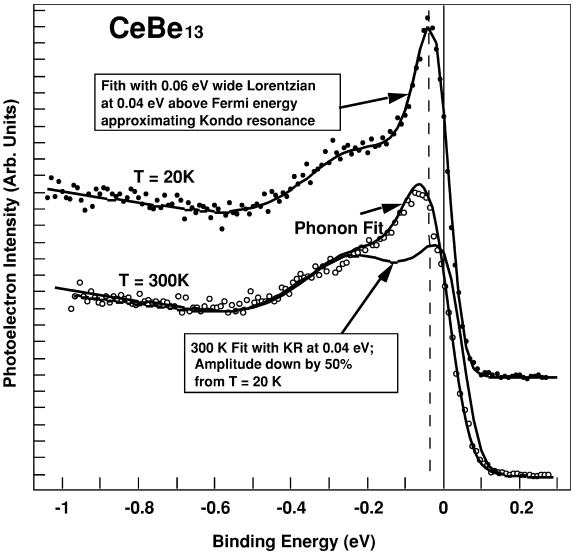

Fig. 3. Near-E_F PES spectra for $CeBe_{13}$ at 20 and 300 K. The 20 K spectrum was fit twice. In the first case a Lorentzian was placed at -20 meV together with background, then broadened, and truncated with a 300 K Fermi function. The result is the 'phonon fit' superimposed on the 300 K data. In the second case a Lorentzian was place at 40 meV above E_F to simulate a KR, decreased in intensity by 50% to simulate the NCA predictions, and then truncated by a 300 K Fermi function. Both fits are equally good at 20 K, but the latter fit yields a shift to the right at 300 K, while the former yields a shift to the left, as per experiment.

for this direction in the Brillouin zone the state is fully occupied and not a mere tail of an intense KR. A background was also included. If this entire fitted lineshape is now convoluted with a Gaussian (FWHM~100 meV) to simulate ~100 meV of phonon broadening, and then convoluted with a 300 K Fermi function, the resulting lineshape fits the 300 K data exactly as shown by the line in the 300 K spectrum, called the photon fit. Convolution with a Fermi function only without broadening is found to be insufficient to fit the 300 K spectrum exactly.

By contrast, 100 meV of broadening (whether due to phonons or other effects — see below) combined with Fermi function convolution are entirely sufficient to explain all temperature effects in Fig. 3, provided that the peak of the narrow DOS feature is below the Fermi energy and fully occupied as assumed in the fits. That this is the case is evidenced by the fact that the peak of the $4f_{7/2}$ shifts toward higher binding energy at 300 K (to the left of the dashed line in Fig. 3). This can only occur if it is fully occupied and broadened, most likely by phonons (but we cannot rule out other broadening mechanisms).

It is however fair to ask whether a similar fit can be obtained with the assumption that the $4f_{7/2}$ is above the Fermi energy and only the tail of this feature is occupied, as would be the case for a KR within NCA. It is straightforward to simulate this case using a Lorentzian centered at 0.04 eV (above E_F) and having a FWHM of 0.06 eV. This new fit is shown in Fig. 3 as the gray line through the $T=20$ K spectrum. The parameters for this Lorentzian are surprisingly close to what one would actually expect for a Kondo resonance in a material having a $T_K \approx$ 400 K so that at first glance it would seem to be consistent with the existence of a KR, and hence the SIM. However, if the temperature is now increased to 300 K, the spectral weight of the Lorentzian representing the KR must be decreased to about half of its intensity [21,22] and the entire spectrum convoluted with a 300 K Fermi function. The result is shown as the dark line spectrum superimposed on the 300 K data. Immediately we see that far too much temperature dependence is predicted, and it would take a severe renormalization of the theory to bring the temperature dependence in line. More importantly, however, the centroid of the simulated peak shows a positive energy shift (to the right of the dashed line) while experimentally the peak actually shifts below the Fermi energy with increasing temperature.

The large amplitude effect and the positive $4f_{5/2}$ peak shift within NCA are a direct consequence of the occupation of only a small tail of a much more intense narrow feature above E_F. It is easy to understand this behavior if the KR (or any sharp feature above E_F) is positioned within k_BT of the 300 K Fermi energy (i.e. within about 20 meV of E_F) and it's width is no more than about 50 meV. At 300 K, the Fermi function samples only about the first 50 meV above E_F. Any DOS beyond that is irrelevant.

The experimental shift away from the Fermi energy, by contrast, is a direct consequence of the broadening of the $4f_{5/2}$ feature. A peak shift can not be obtained if only the Fermi function convolution is used with no phonon broadening (assuming the feature is very sharp). Thus, the observed shift of the peak toward higher binding energies, observed almost universally in Ce heavy fermions, favors the phonon (or other) broadening interpretation.

While we have arbitrarily been calling the broadening effect as phonon broadening, it must be pointed out that the PAM likewise predicts a broadening of PES features with temperature, but not associated with phonons [23,24]. Rather, this is due to a change in the lifetime of the magnetic polarons. Experimentally there is no obvious way to distinguish between phonons and the magnetic polaron interactions inherent in the PAM. Suffice it to say that the temperature effects observed in PES measurements are not from the outset inconsistent with the PAM predictions.

6. $YbInCu_4$: a unique test of the SIM

The heavy fermion compound $YbInCu_4$ has for some time been recognized as possessing perhaps the greatest potential for verification of the applicability of the SIM to stoichiometric, crystalline heavy fermion compounds. It displays an isostructural phase transition [51] at $T_V=42$ K at which, in high quality single crystals, the volume abruptly increases by 0.5% below T_V with no other change in the crystal structure. Only a very slight change in the

s–p–d electronic structure is indicated from PES. The thermodynamically determined Kondo temperature, T_K, changes [51,52] from about 30 K above T_V to about 400 K below T_V. Thus the scaling and other depenencies on T_K are easily tested simply by performing PES measurements above and below T_V. Although a recent paper [53] questioned the usefulness of $YbInCu_4$ as a test for the SIM by introducing the hypothesis that PES measures only a thick subsurface layer and not true bulk electronic states, this hypothesis has recently been shown to be without merit [54]. The unusual temperature dependence found in Ref. [53] is apparently a consequence of defects formed at the transformation. By avoiding defect formation (i.e. PES data are obtained only in a single cooldown of the sample) a clear, abrupt phase transition is observed in the PES spectra. The results are illuminating and discussed below.

Because of the sudden increase in T_K at T_V (from 30 K above T_V to 400 K below T_V) as the temperature is lowered, the spectral changes predicted from NCA [21,2] are that: (A) The hole occupancy, n_h, as determined from thermodynamic measurements, should decrease from 0.99 to 0.9; (B) divalent 4f features (i.e. those shown in Fig. 4) should exhibit a gradual temperature dependent increase in spectral weight as the temperature is lowered, both above and below T_V; (C) the spectral weights of both the $4f_{7/2}$ and the $4f_{5/2}$ should abruptly increase by more than an order of magnitude below T_V; (D) the intrinsic width of the $4f_{7/2}$ should likewise increase by about an order of magnitude; (E) the peak positions of both

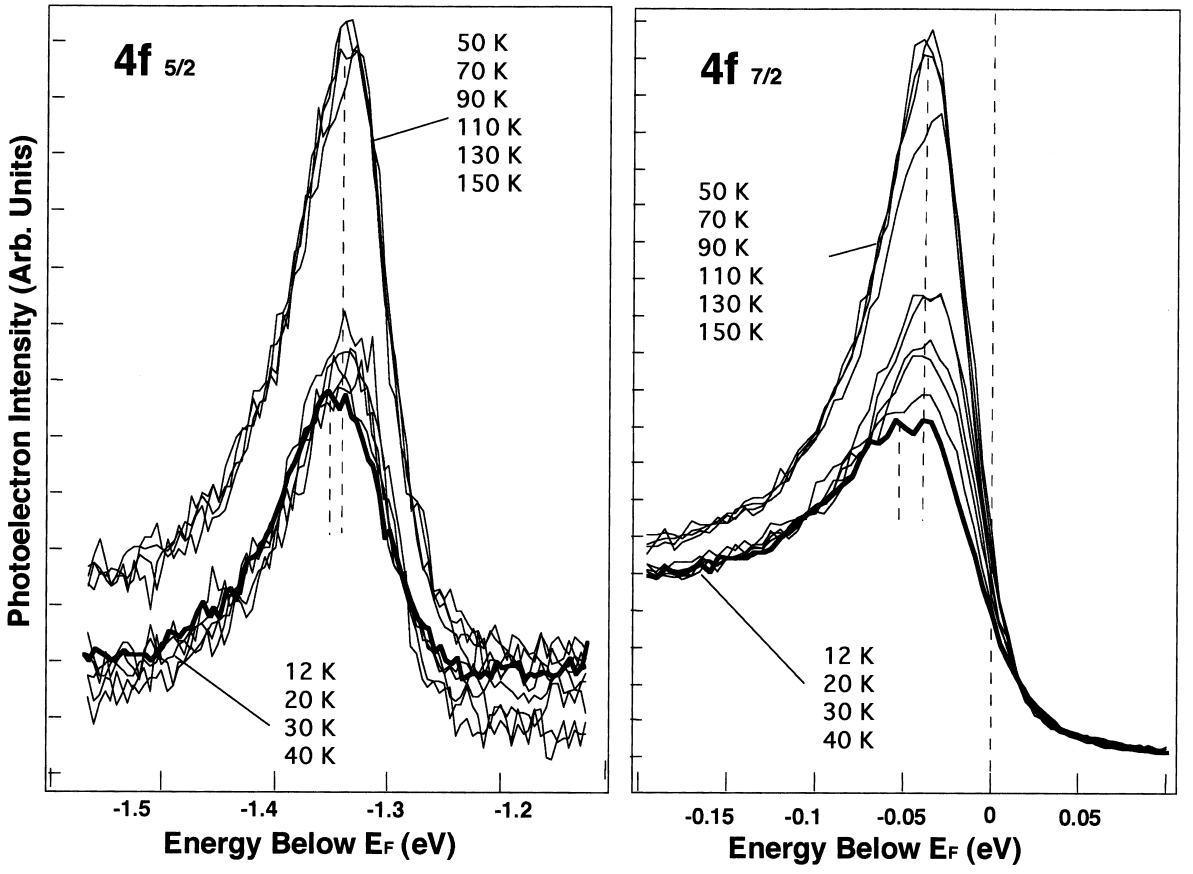

Fig. 4. The bulk divalent $4f_{5/2}$ and $4f_{7/2}$ peaks in the PES spectra of $YbInCu_4$, taken at the indicated temperatures. Note the spectacular grouping of the data into peaks above and below the transition at 42 K. The heavy dark line spectrum corresponds to 150 K where the sample was cleaved. The dashed lines indicate the shift in peak position to the left as T increases (opposite to NCA).

the $4f_{7/2}$ and the $4f_{5/2}$ should shift toward higher binding energy (to the left in Fig. 4) by ~30 meV below T_V. Given the instrument resolution of 25 meV, all these effects are easily tested with a single crystal sample of $YbInCu_4$ cleaved at 150 K and PES spectra measured at various lower temperatures.

An expanded and overlaid view of the divalent bulk $4f_{5/2}$ and $4f_{7/2}$ peaks only is shown in Fig. 4a and b, respectively, for several temperatures above and below T_V (~42 K) at which spectra were taken. The data were normalized to equal total integrated intensities (including the entire valence band region, not shown), with secondary electron features subtracted. The thick-lined spectrum in each frame represents data at 150 K, the highest temperature at which data were taken and at which the sample was cleaved in situ. The grouping of the peaks according to the high-temperature or low-temperature phase is rather striking, and demonstrates a bulk phase transition. No significant temperature effect is observed in the intensities below T_V, with the peaks overlaying each other quite well. Some slight intensity change is seen in the $4f_{5/2}$ peak above T_V, but this can for the most part be accounted for on the basis of phonon broadening discussed above [46,55]. The 150 K spectrum displays a full width at half maximum (FWHM) which is about 10% larger than that observed for the 50 K spectrum (105 vs. 95 meV; i.e. about 50 meV of broadening is evident at 150 vs. 50 K). The 25-meV instrument resolution yields a negligible effect here. By contrast, the $4f_{7/2}$ peak exhibits a clearly discernible increase in intensity above T_V as the temperature is lowered. This, however, is a consequence of the effect of the Fermi function truncation, combined with a convolution of the same 50 meV phonon broadening. The FWHM of the $4f_{7/2}$ increases from about 55 meV at T_V, to about 75 meV at 150 K (including instrument resolution), again representing about 50 meV of phonon broadening, just as in the $4f_{5/2}$. Just above and below T_V there is no change in the FWHM of either the $4f_{5/2}$ or the $4f_{7/2}$. The actual position of the $4f_{7/2}$ is at 40 meV below the Fermi energy, in agreement with Ref. [56], and, perhaps coincidentally, at an energy position consistent with a T_K of 400 K (We say coincidentally because the peak energy is invariant immediately above T_V where NCA would predict a sudden shift. Thus the peak position is perhaps in accidental agreement with NCA below T_V, with serious disagreement above T_V). Since at 150 K we obtain both the 50-meV broadening effect, as well as effects of a Fermi function, whose 10–90% width approaches 60 meV, this significantly reduces the $4f_{7/2}$ peak height as well as yields a gradual, approximately 10 meV, shift of the peak positions (both the $4f_{5/2}$ and the $4f_{7/2}$ undergo a shift; see Ref. [46] for a discussion of this effect) delineated by the dashed lines in Fig. 4a and b. Interestingly (but not surprisingly for a conventional effect), the slow shift with increasing temperature is opposite to the direction one would expect [21,22] from NCA. The hole occupancy, n_h (i.e. essentially the percentage of the total 4f signal that is found in the trivalent configuration of this mixed valent system), was determined in a separate measurement [55] and found to decrease from 0.72 above T_V to 0.6 below T_V. These latter values are not in keeping with the thermodynamically determined values as to bring into question the validity of the SIM (recall the paraphrased statement from Ref. [39]).

With confidence that the features in Fig. 4 represent bulk divalent 4f intensity, the subsurface having been dismissed, let us see how Fig. 4 compares with respect to the NCA predictions delineated above. We consider them point by point in the following:

(A) The hole occupancy, n_h, was measured separately from the data presented in Fig. 4, and is not shown here. It was done at a photon energy of 500 eV where surface features and Cu3d states are substantially diminished so that errors due to non-f background are minimized. It is found that n_h changes suddenly from 0.72 above T_V to 0.6 below T_V. Thus, while the Δn_h is consistent with thermodynamic findings [51,52] at the transition, the absolute values are so out of line that we should not consider $YbInCu_4$ a heavy fermion, but rather a mixed valent system. The NCA approximations are invalid for values of n_h less than about 0.8, perhaps even higher (see the theory section in Ref. [24]). We point all this out forcefully because NCA and the SIM are arbitrarily used by the correlated electron community to model stoichiometric compounds despite its inapplicability.

(B) There is little or no temperature dependence either above or below T_V, except for the small effect arising from Fermi function truncation and broaden-

ing (already discussed with respect to $CeBe_{13}$). This lack of a temperature dependence (except at T_V) has been observed by us in most Yb heavy Fermion systems [24,46]. Indeed, the slight temperature dependence of the $4f_{5/2}$ vs. the $4f_{7/2}$ as a result of Fermi function truncation has been discussed at length in [46] for Yb compounds. While one might argue that in $YbInCu_4$ the lack of a temperature dependence (except at T_V) can be understood if the thermodynamic values of the hole occupancy [51,52], n_h, are applicable (i.e. about 0.9 below T_V and about 0.99 above T_V) on the basis of the fact that below T_V the temperature range is too small to observe an effect while above T_V the n_h is too large (i.e. the material is nearly trivalent) to observe an effect, our measured values of n_h suggests that a large temperature effect should have been observed in both ranges, if NCA were applicable. The problem is two-fold: (1) the PES measured n_h is much too small relative to thermodynamic values of T_K, and (2) given this measured n_h, NCA would predict a large temperature dependence whereas none is observed.

(C) The spectral weight increase below T_V is only about 30% for both the $4f_{7/2}$ and the $4f_{5/2}$, compared to the NCA predicted increase of at least an order of magnitude. This is dramatically shown in Fig. 5 where spectra taken at 12 and 80 K (Fig. 5a) are compared to NCA calculations (Fig. 5b) using parameters consistent with the T_Ks and temperatures shown in the figure. No data manipulation was done in Fig. 5a except for normalization on the background above the Fermi energy (The broad feature at ~ -1 eV is surface related and is to be ignored). The peak intensity above T_V is at least an order of magnitude too large relative to that below T_V. But when absolute values are considered (i.e. when thermodynamic values of n_h are used to calculate intensities) the intensities are as much as a factor of 50 too large relative to NCA.

(D) Just above and below the transition there is no change in the width of either the $4f_{5/2}$ or the $4f_{7/2}$ peaks, while NCA would have the higher temperature $4f_{7/2}$ to be about an order of magnitude narrower than that below T_V. This is not immediately evident from the calculated spectra in Fig. 5b, where spectra were broadened by 70 meV, thus masking the change in width. Even more damaging to NCA and

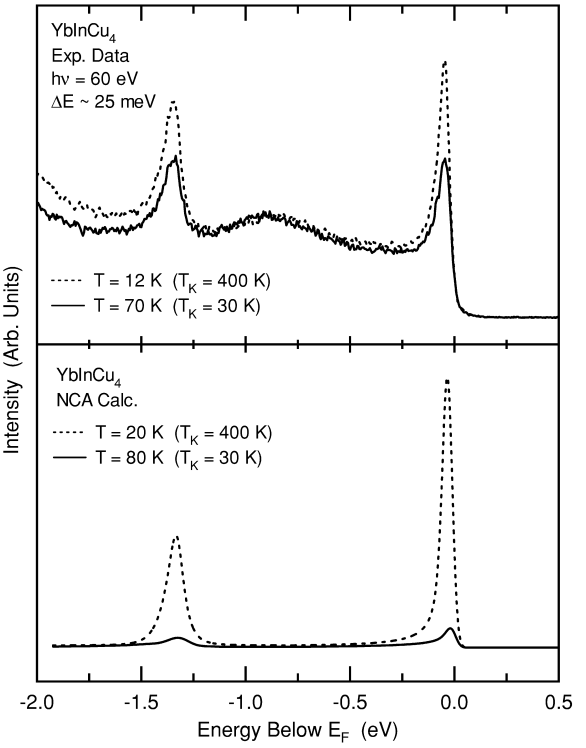

Fig. 5. Upper frame: $YbInCu_4$ spectrum below the transition at 12 K (dashed line) and above the transition at 70 K (solid line). The broad feature at -0.75 is a surface effect to be ignored. Lower frame: NCA calculated spectra assuming the indicated T_Ks. Far too much intensity is observed experimentally. The abrupt shift to the right by 32 meV just above the transition is non-existent.

SIM is the fact that already at 150 K the width of the $4f_{7/2}$ has increased from a FWHM~55 meV in the low temperature phase, to FWHM~75 meV. This is opposite to NCA expectations, but consistent with normal, conventional phonon broadening.

(E) If the thermodynamic values of n_h (i.e. 0.9 and 0.99) were applicable to $YbInCu_4$, then one would expect a shift of the $4f_{5/2}$ and $4f_{7/2}$ peak positions of about 32 meV toward the Fermi energy as the sample transforms (i.e. $\Delta k_B T_K \sim 32$ meV, where $\Delta T_K \sim 370$ K). Experimentally, no shift is observed at the transition. But as the temperature increases toward 150 K, a gradual shift of both the $4f_{5/2}$ and $4f_{7/2}$ occurs in a direction opposite to NCA expectations. By 150 K this shift has reached as much as 10 meV and is shown by the dashed lines in Fig. 4. By

contrast, such a shift is entirely consistent with conventional effects discussed in Ref. [46].

Clearly $YbInCu_4$ does not conform with the SIM and NCA, nor do most stoichiometric heavy fermion compounds. We conclude that the SIM is inapplicable to such materials. At the same time we cannot deny that the SIM successfully explains much of thermodynamic data, and is, at least, internally self-consistent. However, a recent attempt [57] to use parameters obtained from thermodynamic and X-ray (L_{III} edge) data [58] (i.e. T_K, hybridization strength, n_h, etc.), and work backwards from these to obtain a conduction bandwidth, resulted in bandwidths that were at least an order of magnitude too small. Thus while the SIM is internally self-consistent for parameters obtainable via thermodynamic measurements, it fails to provide correct values not measurable by thermodynamic techniques.

7. Models beyond the SIM

It is our contention that the crux of the problem lies in the failure of the SIM to account for the periodic nature of the f-electrons. These f-electrons are not impurities imbedded in a matrix, as in an alloy, but rather they form into Bloch states by way of hybridization with the ligand p or d conduction electrons even at high temperatures. This, of course, is not a new idea, but it has been ignored by much of the correlated electron community owing to the complexities involved in introducing the Anderson Hamiltonian as a perturbation on a band calculation. Moreover, until our high-resolution PES measurements on high-quality single crystals, the existence of narrow f-bands could not be verified. We will show below that the existence of these f-bands can no longer be denied. But we first digress somewhat into possible models that can yield robust narrow bands at temperatures far above the Kondo temperature.

There are a number of models which may eventually prove successful, such as renormalized bands [15,17], LDA + U (many authors), two-electron bands [59], charge polarons investigated by Liu [16], dynamical mean field theory of Kotliar, and the periodic Anderson model (PAM) investigated by Jarrell [23,24]. The latter two models are closely related to each other and to the SIM, but they are not simply an extension of the SIM. They yield new physics. The PAM calculations for model systems have been carried out to a sufficient degree that a number of trends can be gleaned from them. For this reason we elaborate below on the origins and predictions of PAM.

The formation of narrow f-bands within the PAM is based on the Nozieres exhaustion principle [60]. Nozieres argued that since the screening cloud of a local magnetic moment involves conduction electrons within $k_B T_K$ of the Fermi energy, only a fraction of the moments, $n_{eff} \sim \rho_d(0) k_B t_K$ where $\rho_d(0)$ is the conduction electron density at E_F, may be screened by the conventional Kondo effect. The f-moment together with its conduction-band screening cloud forms a spin polaron. Nozieres then proposed that the spin polaron and unscreened sites may be mapped onto particles and holes of a single-band Hubbard model with local Coulomb repulsion U_{ff}. The polarons hop from site to site and effectively screen all the moments in a dynamical fashion. The hopping constant of this effective single-band model is strongly suppressed by the overlap of the screened and unscreened states. Hence the Kondo scale of the effective model, T_{PAM}, becomes much less than T_{SIM}. There are then two temperature scales. This has the effect that for a given thermodynamically measured T_K one has much more hybridization than previously assumed within the SIM (just as we find in our PES data), and one must go to temperatures far above T_K in order for T_{SIM} to be the dominant temperature scale (again, as per our PES data). The PAM is believed to more correctly describe the strong correlation of electrons in Kondo lattice systems. While for more than a decade the SIM has been the paradigm for comparison with PES, it cannot account for the coherent nature of electrons (i.e. periodic Bloch states) now observed both above and below T_K, nor the increased hybridization. The PAM, in principle, accounts for these effects.

Some of the PAM results are consistent with a simple band-formation picture. The model calculations involve an f-level and a d-band in a cubic zone. With no hybridization, the available electronic states consist of a d band and two (doubly degenerate) local f levels separated by U_{ff}. When hybridization, V, is

turned on, a new resonant state forms slightly above the Fermi surface when $n_d<1$, and slightly below when $n_d>1$ (n_d is the conduction band filling which is half filled at $n_d=1$). Much of this is clearly depicted in Fig. 6, where the model calculations are for the metallic state with $n_d<0.8$. The excitation spectra are shown for various momenta in the cubic Brillouin zoner. The results are shown for two temperatures. It is important to note that there is no loss of spectral weight, rather only a broadening effect of the quasiparticle peaks, even at temperatures as high as ten times T_K.

Some of the main conclusions regarding PAM, evident from Fig. 6, then, are the following: (i) The original d-band mixes with the local f-levels and the resonant level, giving rise to a renormalized band which has f character *only* near the renormalized f level energies and has d character far from them. The Kondo states, slightly below the Fermi-level, are only present for **k** near the zone center when $n_d<1$ and **k** near the zone corner when $n_d>1$. They have mostly f character, indicating that the f electrons themselves are involved in screening the local moments through hybridization with the d-band. When screening is almost complete, in the regime of T_{PAM}, a Fermi liquid begins to form. (ii) The PAM predicts a Kondo peak which has a weaker temperature dependence and thus persists up to much higher temperatures (in units of the Kondo scale) compared to the predictions of the SIM. (iii) Both the intensity and the spectral weight of the Kondo peak are larger in the PAM than in the SIM. (iv) In the PAM the Kondo peak intensity does not scale like $1/V$ as in the SIM. (v) The Kondo peak is dispersive in the PAM making a heavy quasi-particle band with strong f-electron character which crosses the Fermi surface and persists up to energies $\gg T_K$ due to a strongly frequency-dependent hybridization function. It should also be repeated that the f-like portion of the PAM bands exists in only a part of the zone: near the zone center when $n_d<1$, and the zone corner when $n_d>1$. For $n_d=1$ the PAM yields an insulating state.

It will be seen below, that the f-character in both magnetic and heavy fermion compounds is indeed

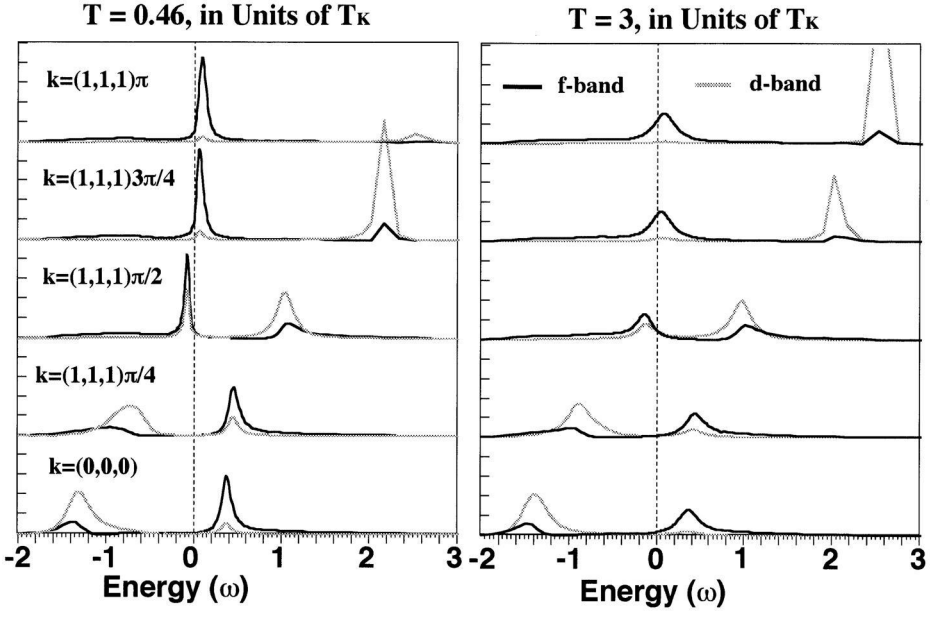

Fig. 6. Excitation spectra for two temperatures calculated from the PAM for various vectors in a cubic zone. Both f and d features are sharp at E_F. But as the band pulls down below E_F it becomes primarily d-like and broad, as found experimentally. At higher temperatures only a broadening effect is predicted.

localized to only a small portion of the zone, and that in uranium compounds the dispersion and hybridization are unmistakable.

8. Experimental evidence for narrow bands

8.1. Ce compounds

Large intensity variations of the $4f_{5/2}$ peak in Ce compounds (the Kondo resonance) which are periodic with the Brillouin zone, were first reported [61] for the compound $CePt_{2+x}$ (where $0<x<1$). These were observed at a temperature (120 K) which exceeded T_K by a factor of more than 10. Actual dispersion of the $4f_{5/2}$, while likely present, was not clearly observed using older electron spectrometers. The same experiment was later repeated by Garnier et al. [62] and, while they did not report dispersion of the $4f_{5/2}$, a careful examination of their data suggests as much as 100 meV of dispersion in the $4f_{5/2}$. The first incontrovertible evidence for dispersion of the $4f_{5/2}$ in Ce compounds was found [44] in $CeBe_{13}$, shown in Fig. 7 for two directions in the zone. The amplitude effects are obvious. The energy shift of the $4f_{7/2}$ actually exceeds 80 meV. Invariably, as the $4f_{5/2}$ feature disperses below the Fermi energy, it broadens, acquires d- or p-character, and loses intensity. Similar results were later seen [63,64] in $CeSb_2$ using 40 eV photons, where the PES p- or d-electron cross sections are significant relative to the f-cross section [65].

It has been suggested that the strong amplitude variations observed in the $Ce4f_{5/2}$ peak are nothing more than photoelectron diffraction in single crystals. This however ignores the fact that the amplitude effect is periodic with the inverse lattice and often associated with a slight dispersion away from the Fermi energy and a broadening of the quasiparticle peaks. Most importantly, however, the amplitude variations are very different for the $4f_{5/2}$ versus the $4f_{7/2}$ peaks (often the $4f_{7/2}$ shows no amplitude

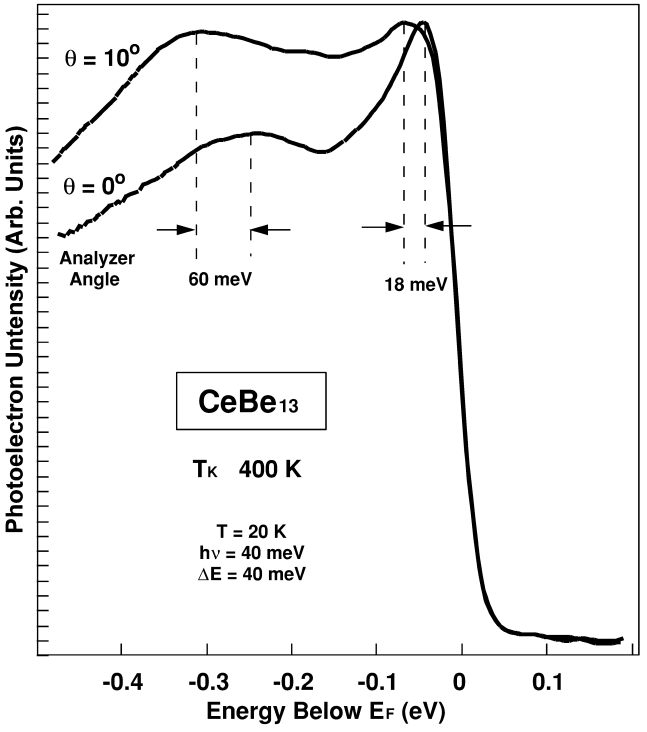

Fig. 7. ARPES spectra at two angles for $CeBe_{13}$ taken at 20 K and $h\nu=40$ eV. Both the KR and the $4f_{7/2}$ disperse significantly. Note how the KR broadens and loses intensity away from E_F.

effect) despite the mere 200 meV separation between them. This argues against photoelectron diffraction in Ce compounds since the two features have the same origin and orbital character and thus would be expected to display identical diffraction effects.

With the development of the Scienta electron energy analyzers it is now possible to collect ARPES spectra with unprecedented energy and angular resolution. This has been utilized in the mapping of the $CeSb_2$ electronic structure (ferromagnetic below 10 K, measured at 20 K; $T_K < 10$ K) which is displayed in the 3D plot in Fig. 8. Color coding (in this and all color figures to follow) is simply a measure of relative intensity, although the highest intensity peaks, red in color, are often associated coincidentally with f-intensity. The longer scans in Fig. 8b capture the f^0 peak at about -2.5 eV, while in Fig. 8a we show an expanded view (1 eV wide scans) near the Fermi energy. Although any dispersion of the $4f_{5/2}$ is less than 10 meV, the amplitudes of both the $4f_{5/2}$ and $4f_{7/2}$ are strongly momentum dependent and do not track with each other. The bulk of the $4f_{5/2}$ intensity is found near the zone corner (near $-6°$ in Fig. 8), indicating, perhaps that $n_p > 1$ (we assume that only p-electrons are available for screening.) Such a localization of the 4f intensity in the zone is possible within the PAM but cannot be explained within the SIM. The f^0 peak at -2.5 eV below E_F, that is to say, the feature which in the SIM is identified with the purely localized trivalent 4f state, actually disperses by as much as 100 meV. The failure to see clear dispersion of the $4f_{7/2}$ in Fig. 8, on the other hand, is understood, assuming p–f hybridized bands, from the following scenario: at $h\nu = 60$ eV, the p-cross section is vanishingly small and we are measuring only the f-portion of the bands. Dispersion, on the other hand, is present only in the region of p-character of the bands. All this is again entirely consistent with the PAM description of correlated behavior in stoichiometric compounds (see conclusion (i) above).

Perhaps the most intriguing feature in Fig. 8 is the band at -0.4 eV, situated just off from the zone center. Clearly this is neither the so-called f^0 peak of Ce compounds nor the spin–orbit split sideband, the $4f_{7/2}$, which is normally observed at about -0.25 eV below E_F. The f^0 peak, to the extent that it is not associated with the surface, is clearly present at -2.5 eV. Photon energy dependence tests show that the PES cross section of the new -0.4 eV feature scales precisely with other 4f-electron features, thus making it a third 4f-band in the spectrum and having about 20 meV of dispersion. At this point there is no explanation for this band within any model, although preliminary LDA calculations suggest a peaking of some f-intensity in this part of the Brillouin zone. In all likelihood, then, this is an LDA-derived feature which probably plays no role in the correlation effects due to being far removed from E_F. Nonetheless it underscores the band formation and indicates that any successful model will probably have to incorporate LDA bands. The PAM, in principle, will do that.

8.2. Yb compounds

In general, Yb compounds display almost undetectable dispersion (10 meV or less) in the $4f_{7/2}$ peak which in Yb compounds is associated with the KR. Nonetheless, the amplitudes of both the $4f_{5/2}$ (at about -1.3 eV) as well as the $4f_{7/2}$ can be strongly momentum dependent. This is most certainly the case in $YbCu_2Si_2$, a heavy fermion compound with $T_K \sim 35$ K. In Fig. 9 we show 3D plots of ARPES spectra obtained for $YbCu_2Si_2$, taken within 3 eV of E_F and using $h\nu = 40$ eV (Fig. 9a) and $h\nu = 60$ eV (Fig. 9b). The instrument resolution is about 25 meV in both plots, even at 60 eV where the 4f-PES cross section dominates. It had previously been demonstrated [46] that bulk 4f features are nearly temperature independent. In Fig. 9b bulk derived 4f intensity dramatically peaks at the zone center where it is much stronger than the surface features, while at $\theta = -12°$, the intensity drops by a factor of 3 to where it is much smaller than the surface states. We assume that these are p–f rather than d–f hybridized

Fig. 8. Three dimensional ARPES spectra for $CeSb_2$ at $h\nu = 60$ eV. (a) Expanded near-E_F view. (b) 4 eV wide scans. Note the concentration of f-intensity near the zone corner ($-6°$). An unexplained 4f feature at -0.4 eV has never been heretofore observed in any heavy fermion system. We associate it with LDA-derived bands.

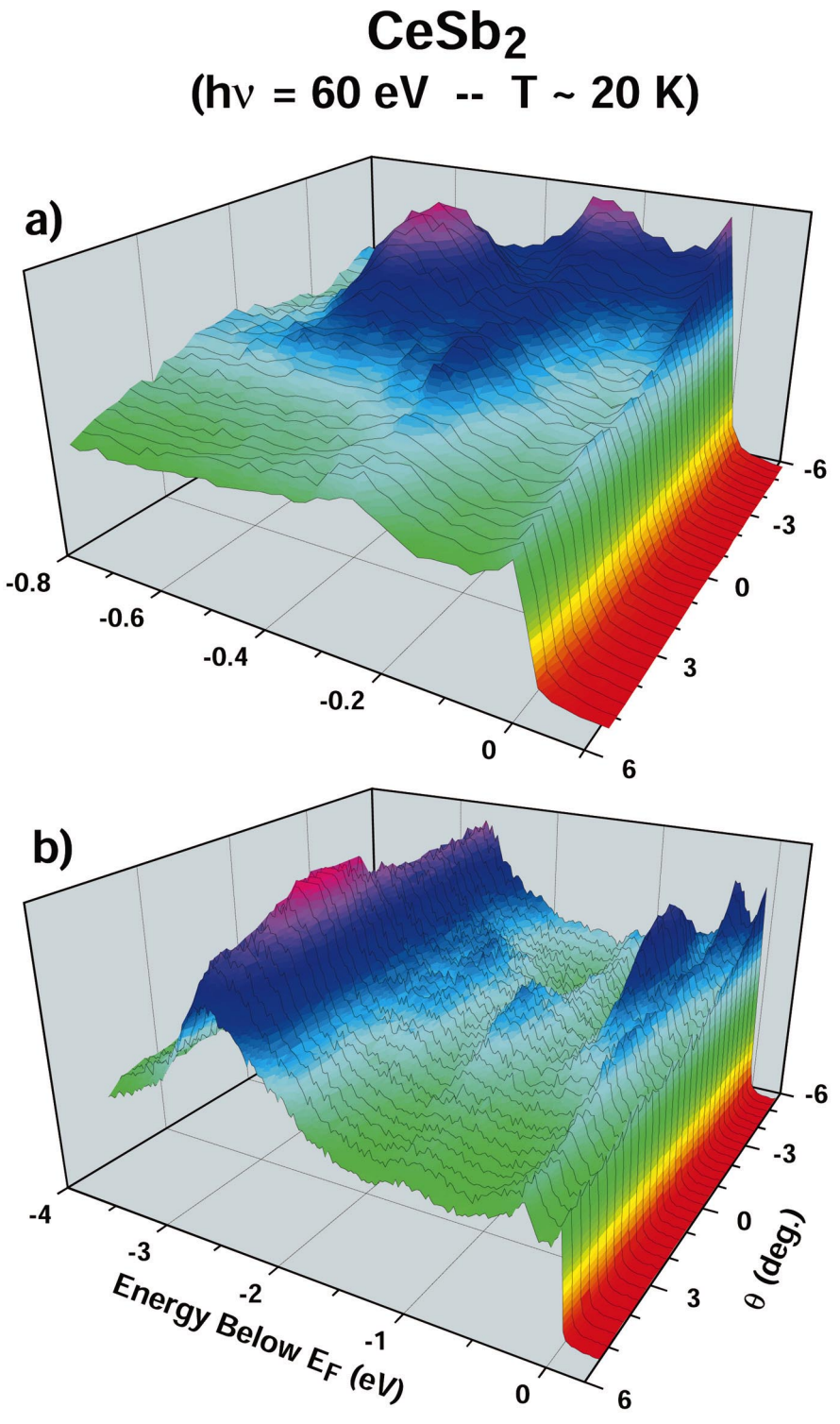
CeSb2
(hν = 60 eV -- T ~ 20 K)
a)
-0.8
-0.6
-0.4
-0.2
0
-6
-3
0
3
6
b)
-4
-3
-2
-1
0
Energy Below EF (eV)
-6
-3
0
3
6
θ (deg.)

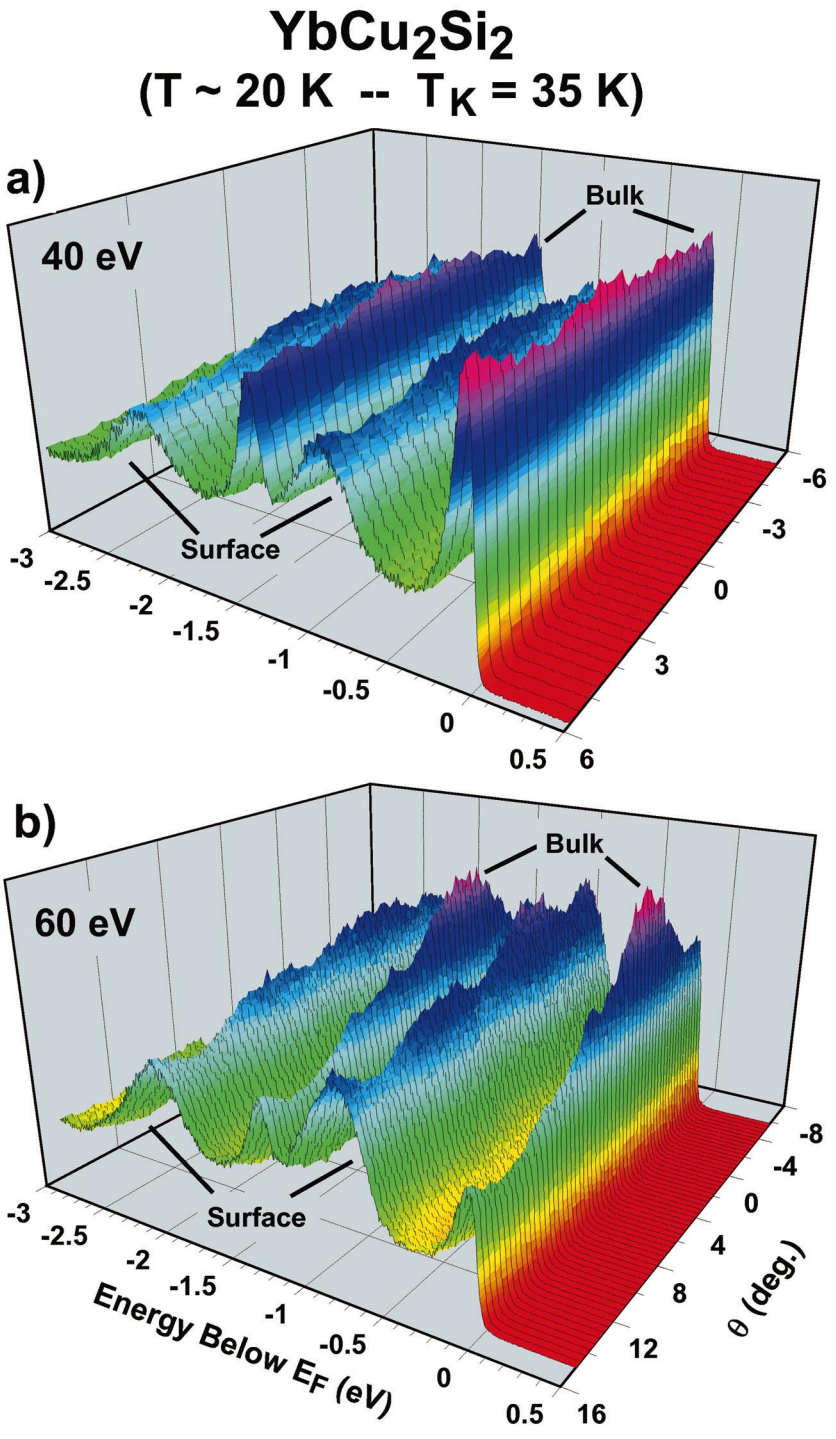

Fig. 9. Three dimensional ARPES spectra for $YbCu_2Si_2$ taken at 20 K and (a) $h\nu = 40$ eV, (b) $h\nu = 60$ eV. The 4f PES cross section dominates at 60 eV where most of the 4f spectral weight is concentrated near the zone center. By contrast, at 40 eV no such concentration is evident probably because the orbital character of the features is more p- or d-like. Note that the surface state intensity is strongly diminished relative to the $4f_{7/2}$.

bands (there are no d-electrons available), and the dispersive p-portion of the bands, if it exists, is not seen due to a vanishingly small cross section. In any case, most of the 4f intensity is concentrated in only a small portion of the zone, amazingly similar to PAM predictions. In Fig. 9a we show the same data but now taken at $h\nu = 40$ eV. The concentration of f-character at the center of the zone is no longer observable. We interpret this as meaning that the orbital character of the features observed at $h\nu = 40$ eV is different from that observed at 60 eV (owing to a smaller f-cross section) and that indeed the feature at E_F is strongly p–f hybridized. At 40 eV we more easily observe the p-electron portion of the near-E_F band, which, surprisingly, is still dispersionless.

The surface features in Fig. 9 are presumed to be more purely 4f-like (the existence of a subsurface is ruled out in Refs. [46,54]). The fact that they are much less intense than the presumably p–f hybridized bulk features at 40 eV is entirely consistent with their lower PES cross section. It is also an argument against photoelectron diffraction (PD) being the source of the amplitude effect since preliminary calculations suggest that the decrease in photon energy (from 60 to 40 eV) is insufficient to cause such dramatic PD effects. It is not possible at this time to completely rule out PD as the source of the amplitude effect in $YbCu_2Si_2$, pending a complete band calculation which is presently in progress. However, based on the similarity to Ce and U compounds, where PD effects are more easily ruled out, we submit that the PAM more effectively explains the momentum dependence in Yb heavy fermions.

The p–f hybridization appears to be pervasive in Yb heavy fermions. In $YbInCu_4$ the dramatic localization of the 4f intensity was not observed, but we nonetheless invoke p–f hybridization in order to explain the photon energy dependence of the $4f_{5/2}$ and $4f_{7/2}$ peaks. In Fig. 10 are shown angle integrated $YbInCu_4$ spectra taken at various photon energies. The interesting fact is that the ratio of the divalent to trivalent signal, while it is more or less constant for all photon energies above 60 eV (up to XPS energies), shows a dramatic change in the 40 eV spectrum. In particular, the trivalent portion of the 4f signal decreases dramatically relative to the bulk divalent signal, so that a determination of the 4f hole

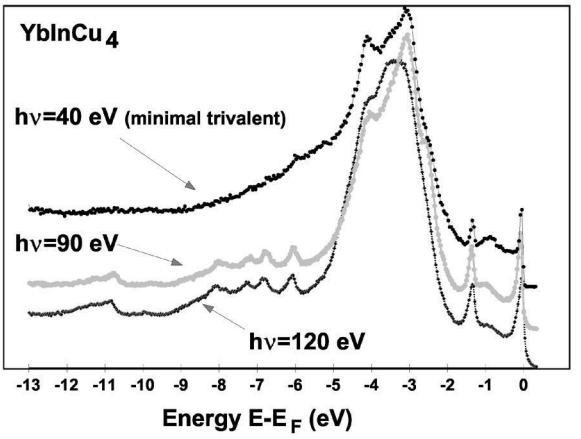

Fig. 10. Angle integrated PES spectra for $YbInCu_4$ at the indicated photon energies. The ratio of the trivalent to divalent intensities is greatly diminished at $h\nu = 40$ eV, most likely due to changing orbital character of the divalent features.

occupancy is no longer valid. Such a decrease occurs in nearly every mixed valent Yb compound that we investigated. Together with this decrease, one usually also observes that the linewidth of the divalent features has narrowed and that the $4f_{7/2}$ gains in intensity relative to the $4f_{5/2}$ (this is also evident in Fig. 9a).

One might at first glance be tempted to ascribe the change in the 4f intensity at 40 eV to surface sensitivity, and hence revive the subsurface scenario. While the arguments for $YbInCu_4$ above have already emphatically ruled out this effect, we point out in addition to the above arguments that the escape depth scenario requires a very gradual change from bulk to subsurface as the kinetic energy of the photoelectrons decreases, unlike the nearly exponential change observed between 40 and 60 eV. If a subsurface were to exist, such that its T_K were much larger than that of the bulk, then for some range of photon energies we should observe two closely spaced divalent features representing the bulk and the subsurface. This is never observed. A more likely interpretation for the rapid decrease in the trivalent intensity relative to the divalent at 40 eV is that the divalent portion of the spectrum consists of ultra-narrow p–f hybridized bands (again, we assume that d–f is unlikely), while the trivalent, or localized portion of the signal, consists of pure 4f states. At

$h\nu = 60$ eV and above (i.e. where the 4f PES cross section is large relative to the p-cross section) one then obtains the same ratio between the divalent and trivalent features. Below 60 eV, on the other hand, the 4f cross section drops exponentially while the p-cross section increases. This results in a quenching of the trivalent signal, while the p-electron portion of the divalent signal gains in intensity. This may explain the observation [66] of Yb4f$_{7/2}$ signal at photon energies as low as 21.2 eV where the 4f cross section should be vanishingly small. Interestingly enough, this non-f intensity is even narrower than the f-intensity. Were it a pure 4f signal due to a higher-T_K subsurface, it would in fact have to be broader. Such a p–f admixture is inconsistent with the predictions of the SIM, but is obtained through the application of the PAM.

8.3. U compounds

Both dispersion and restriction of the f-intensity to only a small portion of the zone are unmistakable in uranium compounds. Indeed, here we observe not only p- or d-electron dispersion, but actual f-electron dispersion. In the case of uranium compounds f–d hybridization is possible since the 6d states are partially occupied and the f-states have a larger spatial extent. We show three representative systems: the heavy fermion UPt_3, the ferromagnet UAsSe, and the antiferromagnet USb_2, all of which display very similar behavior.

ARPES spectra for UPt_3 are shown in Fig. 11, taken with an HAC50 analyzer and thus not shown as 3d plots. The data shown are taken at 20 K, but similar data were obtained at 80 K; i.e. at about 10 times T_K. Various indicated angles are overlaid and it is clear that both the amplitude (only the first 100 meV within E_F are shown) and peak position vary rapidly with angle. Comparison to band calculations [67] shows that the most intense peak, which exists for only the first 3° around the zone center, agrees quite well with the calculated bands. Quite obviously these data will have to be repeated using a Scienta analyzer, but they nevertheless show the essential features of narrow bands and similarity to LDA bands. They will have to be repeated as well due to the fact that the data in Fig. 11 are taken at $h\nu = 30$ eV which argues for a substantial p- or d-admixture.

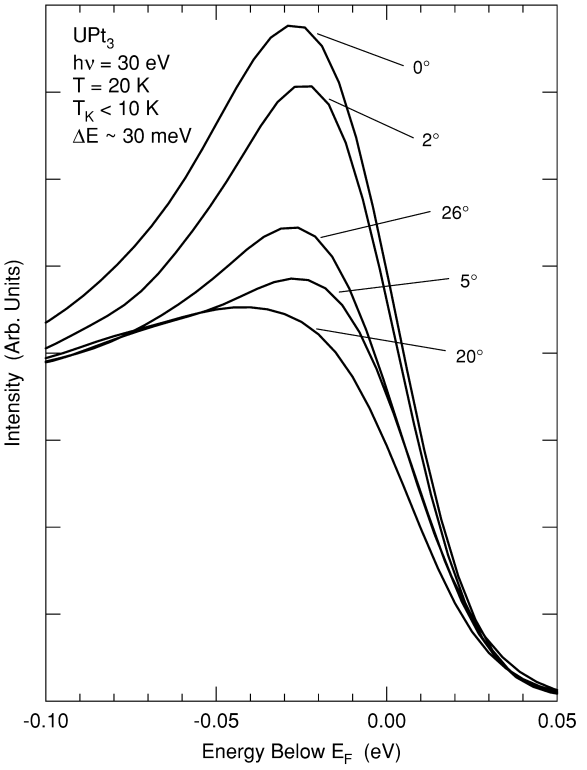

Fig. 11. ARPES spectra for UPt3 for several analyzer settings using $h\nu = 30$ eV at 20 K. Both peak positions and intensities change dramatically with a mere 3° change in emission angle from 2 to 5°.

The use of the high-resolution Scienta is again far more illuminating. Color three-dimensional ARPES spectra for the ferromagnet UAsSe ($T_C = 113$ K, data taken at 20 K, instrument resolution = 25 meV) are shown in Fig. 12 for data taken at $h\nu = 40$ eV (Fig. 12a), where the PES cross section favors p- or d-emission, and $h\nu = 60$ eV (Fig. 12b) where the cross section favors primarily f-emission. Only the first 200 meV of states below E_F are shown. There is again a dramatic difference between the two frames. Indeed, the strong f-intensity in Fig. 12b (again localized to only a small portion of the zone; near the zone corner along the Γ–X direction) appears precisely in the location where in Fig. 12a the d-intensity (we assume we are dealing here with uranium 6d electrons) has a deep minimum. Here the 5f portion of the band actually shows dispersion to the tune of about 50 meV, rather than just intensity

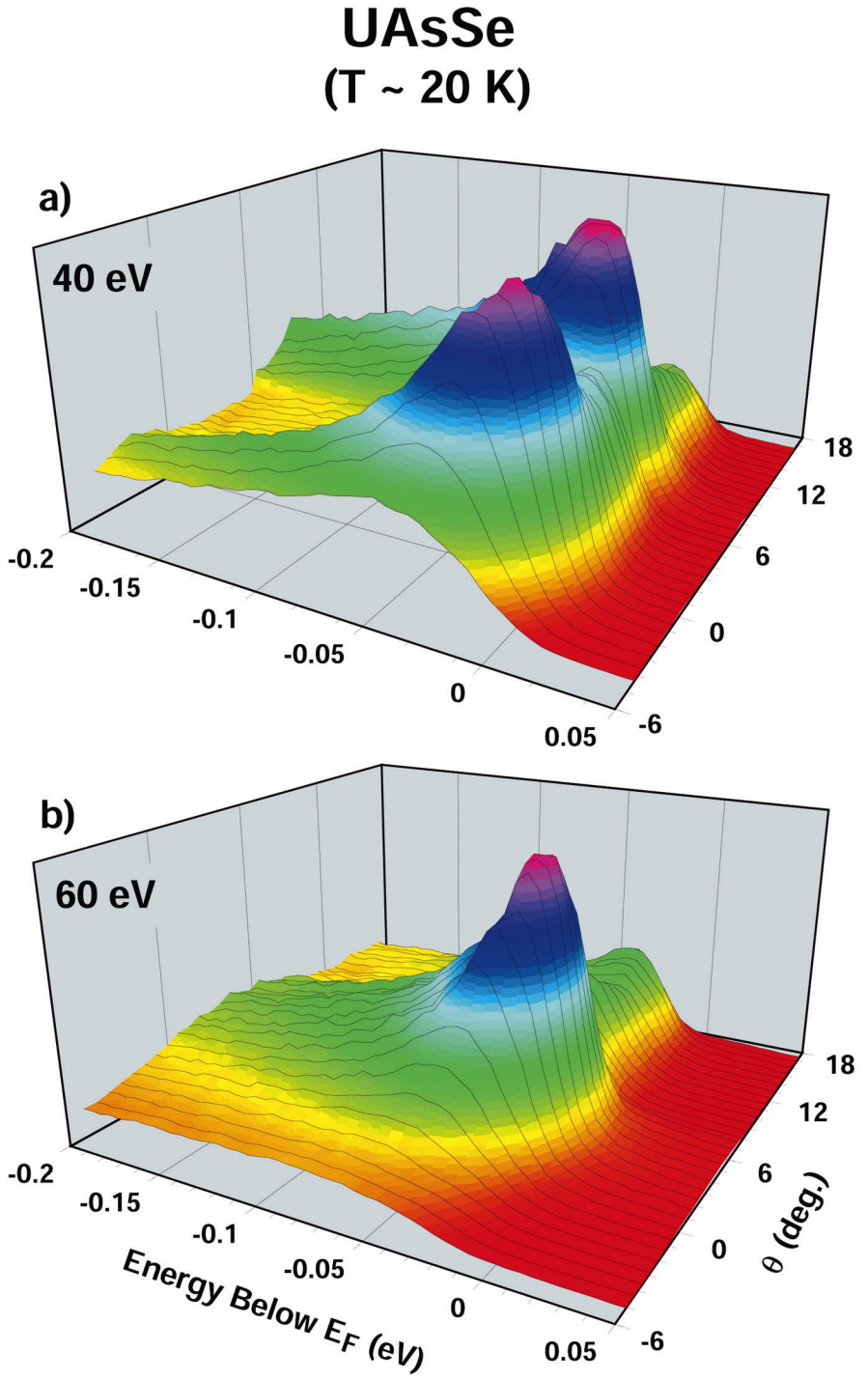

Fig. 12. Three dimensional ARPES spectra within 200 meV of E_F for ferromagnetic UAsSe at: (a) $h\nu = 40$ eV, emphasizing d-emission, and (b) $h\nu = 60$ eV, emphasizing f-emission. The strong f-electron feature in (b) fits precisely in the notch of the d-bands in (a) — a classic example of f–d hybridization. The pure f-electron band in (b) disperses by ~50 meV.

modulation. This is a classic example of d–f hybridization. The measured bands agree almost exactly with the calculated bands of Oppeneer et al. [68], with the exception that they appear to be strongly renormalized (much narrower) at the Fermi energy vs. calculations. This again would seem consistent with the expectations from the PAM, although calculations for real systems are not yet forthcoming. The excellent agreement with band calculations as to the location of the 5f states would also argue strongly against PD as the source of the large intensity variation of the 5f signal. It would be indeed pathological that PD would fortuitously yield an amplitude diminution precisely at those momenta where band calculations predict the change in orbital character from f to d.

The magnetic moment almost surely must be carried by the strongly hybridized f-band at the Fermi energy and we are clearly dealing with band magnetism. The ordered moment is measured to be 2.5 μ_B which is only slightly below the purely localized case. What is surprising is that the f-band occupies such a small part of the zone. Based on band calculations, the f-band actually crosses E_F.

Finally we consider the the antiferromagnet USb_2, whose ARPES spectra, taken with a Scienta and shown in color 3D, are depicted in Fig. 13. The Neel temperature for this material is 200 K while our measurements were done at 20 K to avoid Fermi function smearing. Three frames are shown in Fig. 13, for data taken at $h\nu=33$ eV (Fig. 13a), 40 eV (Fig. 13b), and 60 eV (Fig. 13c), so that we emphasize p-electrons, d-electrons, and f-electrons, respectively. Quite obviously in Fig. 13a the sharp peak (most likely of p-electron origin) is at the Fermi energy, but appears to dissipate at $\theta=0$; i.e. near the center of the Brillouin zone where it begins to hybridize with the f-states. By contrast, in Fig. 13c, the f-intensity at the Fermi energy begins to build precisely where the p-intensity is waning. Thus we conclude that we have again a classic case, this time of p–f hybridization, with the f-portion of the band showing unmistakable dispersion.

Interestingly enough, the d-like portion of the spectrum, which should be emphasized at 40 eV in Fig. 13b, is actually a separate band, slightly removed (by about 100 meV) from the Fermi energy, and in this case does not seem to hybridize with the f-electrons. Again, then, we are dealing with band antiferromagnetism which is somewhat reflected in its ordered moment of about 1.89 μ_B. Once again, too, the f-intensity is confined to the center of the Brillouin zone, making once again reasonable contact with the PAM.

Realizing that it is difficult to observe 5f dispersion in Figs. 12 and 13, we show in Fig. 14 a blowup of the first 100 meV of the ARPES spectra taken at $h\nu=60$ eV for both UAsSe and USb_2. Here it is trivial to see the 5f dispersion and the decrease of intensity as the bands change character to d-like away from the Fermi energy.

It might be useful to point out that most of the results shown here can serve as a warning to those performing measurements on f-electron systems using only HeI or HeII radiation. The above results show that they may be measuring only the p- or d-portion of the hybridized f-bands, which could easily mislead interpretation. At the very least, the determination of n_h values in Yb compounds, where correct f-spectral weights are crucial, should only be attempted at photon energies above 60 eV.

9. Conclusions

We have shown with numerous examples that there is a common theme regarding the electronic structure of stoichiometric heavy fermion compounds; namely, there exist at E_F very narrow, possibly renormalized, p–f or d–f hybridized bands. These are clearly observable in uranium compounds via f-electron band dispersion, while in Ce and Yb compounds the momentum dependence of the amplitude constitutes the main evidence. Spectroscopic data on $YbInCu_4$ demonstrate that the SIM predictions fail, and most likely some version of the PAM is needed. As pointed out by Jarrell, the PAM is not merely an extension of the SIM, but rather introduces new physics which is in better agreement with PES data. The successful model will have to incorporate LDA bands which in UAsSe are in agreement with ARPES results — except at E_F, where they are flatter. The existence of f-spectral weight in only a small portion of the Brillouin zone would seem to agree with the predictions of the PAM as discussed in [24]. In all cases it appears that as the

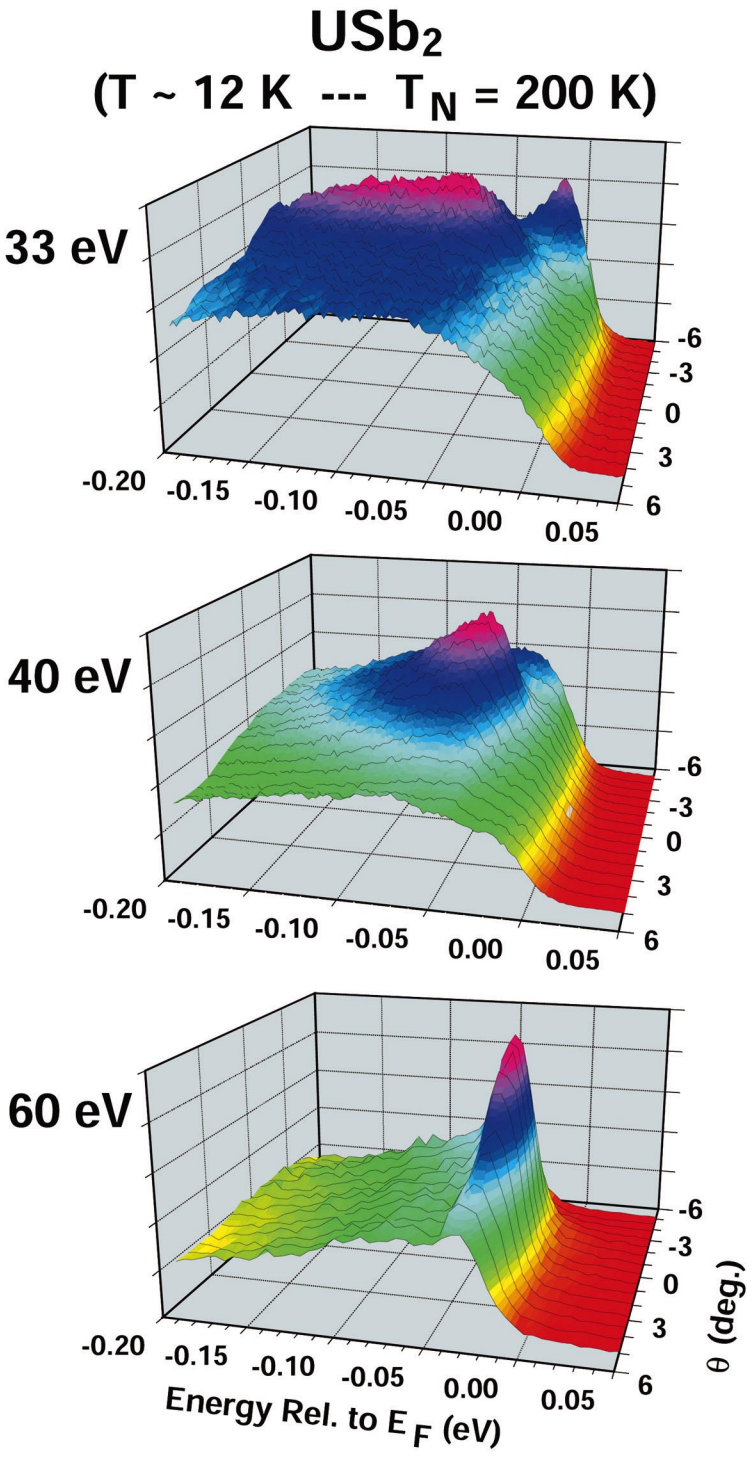

Fig. 13. ARPES spectra within 200 meV of E_F for antiferromagnetic USb_2 at three photon energies: (a) 33 eV, emphasizing p-emission (b) 40 eV, emphasizing d-emission, and (c) 60 eV emphasizing f-emission. The dispersive pure f-band in (c) smoothly diminishes and becomes the p-band in (a). The d-band in (b) is a separate band and is not hybridized with the f-states.

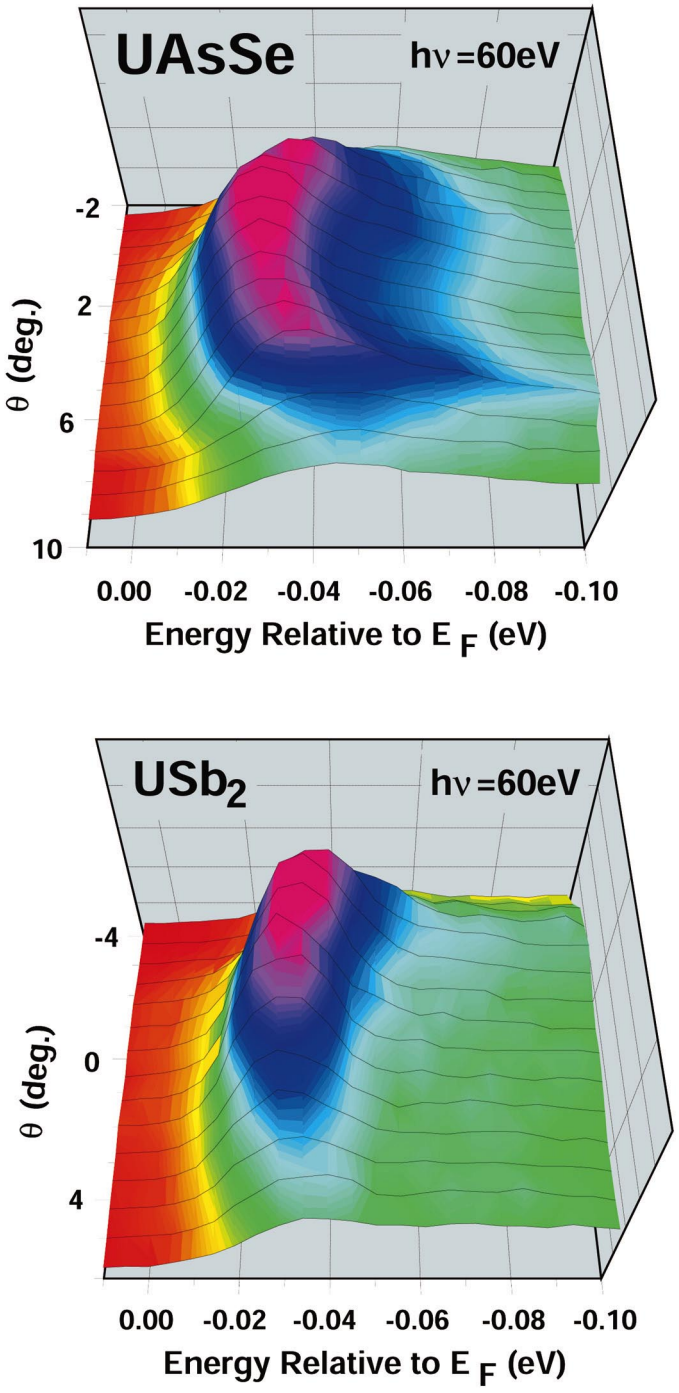

Fig. 14. ARPES spectra for UAsSe and USb_2 within the first 100 meV of the Fermi energy in order to more clearly display the dispersion of the 5f bands. The photon energy is 60 eV where the photoemission cross section for 5f states is near its maximum while the p- and d-electron cross sections are suppressed.The loss of intensity as the 5f bands disperse away from the Fermi energy is indicative of hybridization with p- or d-electrons.

f-band hybridizes with a p- or a d-band, it pulls away from the Fermi energy, broadens, and decreases in intensity. The use of only HeI or HeII radiation may often fail to fully probe these f-states. Only above $h\nu = 60$ eV does the PES f-cross section dominate in cases where the bands are hybridized. For this reason a determination of n_h in Yb compounds is questionable below $h\nu = 60$ eV.

Acknowledgements

This work was supported by the US Department of Energy, Office of Basic Energy Sciences, Division of Materials Science. The work was performed at the Synchrotron Radiation Center of the University of Wisconsin, which is operated by the National Science Foundation under Award ≠DMR-0084402.

References

[1] K. Andres, J.E. Graebner, H.R. Ott, Phys. Rev. Lett. 35 (1975) 1779.
[2] F. Steglich et al., Phys. Rev. Lett. 43 (1979) 1892.
[3] Z. Fisk, J.L. Sarrao, J.L. Smith, J.D. Thompson, Proc. Natl. Acad. Sci. USA 92 (1995) 6663.
[4] N. Grewe, F. Steglich, in: K.A. GschneidnerJr., L. Eyerling (Eds.), Handbook on the Physics and Chemistry of the Rare Earths, Vol. 14, North-Holland, Amsterdam, 1991, pp. 343–474.
[5] D.W. Hess, P.S. Riseborough, J.L. Smith, in: G.L. Trigg (Ed.), Encyclopedia of Applied Physics, Vol. 7, VCH, New York, 1993, pp. 435–463.
[6] H.R. Ott, Z. Fisk, in: A.J. Freeman, G.H. Lander (Eds.), Handbook on the Physics and Chemistry of the Actinides, North-Holland, Amsterdam, 1987, pp. 85–225.
[7] G.R. Stewart, Rev. Mod. Phys. 56 (1984) 755.
[8] J.D. Thompson, J.M. Lawrence, in: K.A. GschneidnerJr., L. Eyerling (Eds.), Handbook on the Physics and Chemistry of the Rare Earths, Vol. 19, North-Holland, Amsterdam, 1994, pp. 383–478.
[9] J.W. Allen, S.-J. Oh, O. Gunnarson, K. Schonhammer, M.B. Maple, M.S. Torikachvili, I. Lindau, Adv. Phys. 35 (1986) 275.
[10] M. Springford, P.H.P. Reinders, J. Magn. Magn. Mater. 76–77 (1988) 11.
[11] G.G. Lonzarich, J. Magn. Magn. Mater. 76–77 (1988) 1.
[12] Y. Onuki, Physica B 186–188 (1993) 92.
[13] P.A. Lee, T.M. Rice, J.W. Serene, L.J. Sham, J.W. Wilkins, Commun. Condens. Mater. Phys. 12 (1986) 99.
[14] J.M. Lawrence, P.S. Riseborough, R.D. Parks, Rep. Prog. Phys. 44 (1981) 1.
[15] G. Zwicknagl, Adv. Phys. 41 (1992) 203.
[16] S.H. Liu, in: Handbook on the Physics and Chemistry of Rare Earths, Vol. 17, North Holland, Amsterdam, 1993, pp. 87–148, Chapter 111.
[17] P. Strange, D.M. Newns, J. Phys. F 16 (1986) 335.
[18] O. Gunnarson, K. Schonhammer, in: T. Kasuya, T. Saso (Eds.), Theory of Heavy Fermions and Valence Fluctuations, Springer, Berlin, 1986, p. 110.
[19] O. Gunnarsson, K. Schonhammer, in: K.A. GschneidnerJr., L.J. Eyring, S. Huffner (Eds.), Handbook of Physics and Chemistry of Rare Earths, Vol. 10, Elsevier, Amsterdam, 1987.
[20] N.E. Bickers, Rev. Mod. Phys. 59 (1987) 845.
[21] N.E. Bickers, D.L. Cox, J.W. Wilkins, Phys. Rev. Lett. 54 (1985) 230.
[22] N.E. Bickers, D.L. Cox, J.W. Wilkins, Phys. Rev. B 36 (1987) 2036.
[23] A.N. Tahvildar-Zadeh et al., Phys. Rev. B 55 (1997) R3332.
[24] A.J. Arko et al., in: K.A. Gschneidner, L. Eyring (Eds.), Handbook on the Physics and Chemistry of the Rare Earths, Vol. 26, Elsevier, Amsterdam, 1999, pp. 265–382.
[25] J.W. Allen, in: R.Z. Bachrach (Ed.), Synchrotron Radiation Research: Advances in Surface and Interface Science, Techniques, Vol. I, Plenum Press, New York, 1992, pp. 253–323.
[26] F. Patthey, B. Delley, W.D. Schneider, Y. Baer, Phys. Rev. Lett. 55 (1985) 1518.
[27] F. Patthey, J.-M. Imer, W.-D. Schneider, H. Beck, Y. Baer, Phys. Rev. B 42 (1990) 8864.
[28] F. Patthey, W.-D. Schneider, Y. Baer, B. Delley, Phys. Rev. Lett. 58 (1987) 2810.
[29] F. Patthey, W.D. Schneider, M. Grioni, D. Malterre, Y. Baer, Phys. Rev. Lett. 70 (1993) 1179.
[30] F. Patthey, W.D. Schneider, Y. Baer, B. Delley, Phys. Rev. B 34 (1986) 2967.
[31] F. Patthey, W.D. Schneider, Y. Baer, B. Delley, Phys. Rev. B 35 (1987) 5903.
[32] D. Malterre, M. Grioni, P. Weibel, B. Dardel, Y. Baer, Phys. Rev. Lett. 68 (1992) 2656.
[33] D. Malterre, M. Grioni, P. Weibel, B. Dardel, Y. Baer, Europhys. Lett. 20 (1992) 445.
[34] D. Malterre, M. Grioni, P. Weibel, B. Dardel, Y. Baer, Phys. Rev. Lett. 68 (1992) 2656.
[35] D. Malterre, M. Grioni, P. Weibel, B. Dardel, Y. Baer, Physica B 199 (1994) 76.
[36] D. Malterre et al., Adv. Phys. 45 (1996) 299.
[37] D. Maltterre, M. Grioni, P. Weibel, B. Dardel, Y. Baer, Phys. Rev. B 48 (1993) 10599.
[38] L.H. Tjeng, S.-J. Oh, C.T. Chen, J.W. Allen, D.L. Cox, Phys. Rev. Lett. 72 (1994) 1775.
[39] L.H. Tjeng, S.-J. Oh, E.-J. Cho, H.-J. Lin, C.T. Chen, G.-W. Gweon, J.-H. Park, J.W. Allen, T. Suzuki, M.S. Makivic, D.L. Cox, Phys. Rev. Lett. 71 (1993) 1419.
[40] P. Weibel, M. Grioni, D. Malterre, B. Dardel, Y. Baer, M. Besnus, Z. Phys. B 91 (1993) 337.
[41] J.S. Kang, J.W. Allen, O. Gunnarsson, N.E. Christensen, O.K. Anderson, Phys. Rev. B 41 (1990) 6610;
L.Z. Liu, J.W. Allen, O. Gunnarsson, N.E. Christensen, O.K. Anderson, Phys. Rev. B 45 (1992) 8934.

[42] L.-Z. Liu, J.W. Allen, C.L. Seaman, M.B. Maple, Y. Dalichaouch, J.-S. Kang, M.S. Torikachvili, M.L. Lopez de la Torre, Phys. Rev. Lett. 68 (1992) 1034.
[43] L.Z. Liu, J.W. Allen, O. Gunnarsson, N.E. Christensen, O.K. Anderson, Phys. Rev. B 45 (1992) 8934.
[44] A.B. Andrews, J.J. Joyce, A.J. Arko, Z. Fisk, P.S. Riseborough, Phys. Rev. B 53 (1996) 3317.
[45] R.I.R. Blyth, J.J. Joyce, A.J. Arko, P.C. Canfield, Z. Fisk, J.D. Thompson, R.J. Bartlett, J. Tang, J.M. Lawrence, Phys. Rev. B 48 (1993) 9497.
[46] J.J. Joyce, A.B. Andrews, A.J. Arko, R.I.R. Blyth, R.J. Bartlett, C.G. Olson, D.M. Poirier, P.C. Canfield, P.J. Benning, Phys. Rev. B 54 (1996) 17515.
[47] A.J. Arko, J.J. Joyce, J. Sarrao, Z. Fisk, J.L. Smith, J.D. Thompson, M. Hundley, A. Menovsky, A. Tahvildar-Zadeh, M.A. Jarrel, in: A. Gonis, N. Kioussis, M. Ciftan (Eds.), Electron Correlations and Materials Properties, Kluwer/Plenum Press, New York, 1999, pp. 33–58.
[48] J.J. Joyce, A.J. Arko, J.L. Sarrao, K.S. Graham, Z. Fisk, P.S. Riseborough, Philos. Mag. 79 (1999) 1.
[49] J.J. Yeh, I. Lindau, At. Data Nucl. Data Tables 32 (1985) 1.
[50] J.J. Joyce, A.J. Arko, Phys. Rev. Lett. 70 (1993) 1181.
[51] I. Felner, I. Nowik, Phys. Rev B 33 (1986) 617;
I. Felner et al., Phys. Rev B 35 (1987) 6956;
I. Nowik et al., Phys. Rev B 37 (1988) 5633.
[52] J.L. Sarrao, C.D. Imer, C.L. Benton, Z. Fisk, J.M. Lawrence, D. Mandrus, J.D. Thompson, Phys. Rev B 54 (1996) 12207.
[53] F. Reinert, R. Claessen, G. Nicolay, D. Ehm, S. Huffner, W.P. Ellis, G.-H. Gweon, J.W. Allen, B. Kindler, W. Assmus, Phys. Rev. B 58 (1998) 12808.
[54] D.P. Moore, J.J. Joyce, A.J. Arko, J.L. Sarrao, L. Morales, H. Hochst, Y.D. Chuang, Phys. Rev. B 62 (2000) 16492.
[55] J.J. Joyce, A.J. Arko, L. Morales, J.L. Sarrao, H. Hochst, Phys. Rev. B (Comment accepted, awaiting reply from authors of Ref. [53]).
[56] S. Huffner, R. Claessen, F. Reinert, Th. Straub, V.N. Strocov, P. Steiner, J. Electron Spectrosc. Relat. Phenom. 100 (1999) 191.
[57] J.L. Sarrao, C.D. Imer, Z. Fisk, C.H. Booth, E. Figueroa, J.M. Lawrence, R. Modler, A.L. Cornelius, M.F. Hundley, G.H. Kwei, J.D. Thompson, F. Bridges, Phys. Rev. B 59 (1999) 6855.
[58] J.M. Lawrence, R. Osborn, J.L. Sarrao, Z. Fisk, Phys. Rev. B 59 (1999) 1134.
[59] Q.G. Sheng, B.R. Cooper, Philos. Mag. Lett. 72 (1995) 123.
[60] P. Nozieres, Ann. Phys. 10 (1985) 19.
[61] A.B. Andrews, J.J. Joyce, A.J. Arko, J.D. Thompson, J. Tang, J.M. Lawrence, J.C. Hemminger, Phys. Rev. B 51 (1995) 3277.
[62] M. Garnier, D. Purdie, K. Breuer, M. Hengsberger, Y. Baer, Phys. Rev. B 36 (1997) R11399.
[63] A.J. Arko, J.J. Joyce, L.E. Cox, L. Morales, J. Sarrao, J.L. Smith, Z. Fisk, A. Menovsky, A. Tahvildar-Zadeh, M. Jarrell, J. Alloys Comp. 1 (1998) 1.
[64] A.J. Arko, J.J. Joyce, A.B. Andrews, J.D. Thompson, J.L. Smith, D. Mandrus, M.F. Hundley, A.L. Cornelius, E. Moshopoulou, Z. Fisk, P.C. Canfield, A. Menovsky, Phys. Rev. B 56 (1997) R7041.
[65] J.J. Yeh, I. Lindau, At. Data Nucl. Data Tables 32 (1985) 1.
[66] S. Huffner, R. Claessen, F. Reinert, Th. Straub, V.N. Strocov, P. Steiner, J. Electron Spectrosc. Relat. Phenom. 100 (1999) 191.
[67] R.C. Albers, A.M. Boring, N.E. Christensen, Phys. Rev. B 133 (1986) 8116.
[68] P. Oppeneer, M.S.S. Brooks, V.N. Antonov, T. Kraft, H. Eschring, Phys. Rev. B 53 (1997) R10437.